Luminescent Langmuir−Blodgett Films of Platinum(II) Complex [Pt(L18)Cl](PF_6) (L18 = 2,6-Bis(1-octadecylbenzimidazol-2-yl)pyridine)

Kezhi Wang,[†,#] Masa-aki Haga,*[,†] Hideaki Monjushiro,[‡] Masaharu Akiba,[§] and Yoichi Sasaki[§]

Department of Applied Chemistry, Faculty of Science and Engineering, Chuo University, 1-13-27 Kasuga, Bunkyo-Ku, Tokyo 112-8551, Japan, Department of Chemistry, Graduate School of Science, Osaka University, Toyonaka, Osaka 560-0043, Japan, and Division of Chemistry, Graduate School of Science, Hokkaido University, Kita-ku, Sapporo 060-0810, Japan

Received July 26, 1999

A novel amphiphilic Pt complex containing 2,6-bis(1-octadecylbenzimidazol-2-yl)pyridine (L18), [Pt(L18)Cl](PF_6), has been synthesized. The complex exhibits concentration-dependent absorption and emission spectra in solution. With increasing the concentration of the Pt complex, we observed a new absorption band centered at 550 nm derived from a metal−metal dσ* to ligand π* charge transfer (MMLCT) transition and the corresponding broad emission centered at 650 nm. The Pt complex is surface-active, and the surface pressure−area isotherm reveals three phase transitions. The three phases correspond to one liquid-expanding phase and two solid-condensed phases, respectively, with different intermolecular overlap in the "flat-on" orientation at the air−water interface. Without additives such as fatty acids, the complex forms a stable and reproducible Langmuir−Blodgett (LB) multilayer film above a surface pressure of 15 mN m^{-1}. Strong emission from the LB films, even monolayer, was observed. Comparing the relative emission intensity of the MMLCT band for transferred LB monolayer film with that for cast films, we concluded that Pt−Pt interactions are suppressed in the LB film. Instead, the emission at 600 nm arising from the ligand−ligand $\pi-\pi$ interacted excited state became dominant. The results would provide the insight into the control of molecular ordering for planar Pt complexes from the viewpoint of characteristic excited states.

Introduction

Square-planar d^8 complexes show a pronounced tendency to stack into one-dimensional (1D) chain polymers. The one-dimensional solids exhibit anisotropic physical properties such as conductivities and optical properties.[1] A well-known example of the synthesis of this type of 1D Pt complex is Magnus's green salt, which was prepared by the mixing of $[Pt(NH_3)_4]^{2+}$ and $[PtCl_4]^{2-}$. Furthermore, the simple crystallization of Pt(II) complexes sometimes leads to 1D chain structures having Pt−Pt interactions.[2−4] In these two methods the 1D structures were obtained by chance and are hard to synthesize in a controllable manner. Our purpose in conducting this study is to control the Pt−Pt interaction and the molecular ordering of square-planar Pt complexes by using Langmuir−Blodgett (LB) techniques at the air−water interface since a two-dimensional environment at the air−water interface will be suitable for controlling the formation of oriented molecular assemblies. LB studies on Pt complexes have been reported by DeArmond et al.[5,6] The square-planar Pt complex $Pt(Thpy)_2$ (Thpy = 2-(2-thienyl)-2-pyridine) shows two molecular orientations: i.e., flat-on (horizontal) and side-on (vertical) orientations depending on the surface pressures in a mixture of $Pt(Thpy)_2$/stearic acid. Recently, anisometric cyclometalated Pt(II) complexes with longer alkyl chains have been synthesized in order to obtain the liquid crystal mesogenic assemblies.[7] Another new class of one-dimensional supramolecular assembly was prepared by the combination of cationic halide-bridged mixed-valence platinum complex and anionic amphiphiles.[8]

Pt(II) diimine complexes often possess emissive excited states, although the studies revealed varieties of lowest energy excited triplet states such as diimine ligand-localized (^{3}IL), metal-to-ligand charge transfer (^{3}MLCT), ligand-to-ligand charge transfer, and metal−metal dσ* to ligand π* charge transfer (MMLCT) excited states.[4,9−16] Several mononuclear complexes have

* To whom correspondence should be addressed. E-mail: mhaga@apchem.chem. chuo-u.ac.jp.
[†] Chuo University.
[‡] Osaka University.
[§] Hokkaido University.
[#] Current address: Chemistry Department, Beijng Normal University, P. R. China.

(1) Okamoto, H.; Yamashita, M. *Bull. Chem. Soc. Jpn.* **1998**, *71*, 2023.
(2) Chan, C.-W.; Lai, T.-F.; Che, C.-M.; Peng, S.-M. *J. Am. Chem. Soc.* **1993**, *115*, 11245.
(3) Ratilla, E. M. A.; Scott, B. K.; Moxness, M. S.; Kostic, N. M. *Inorg. Chem.* **1990**, *29*, 918.
(4) Bailey, J. A.; Hill, M. G.; March, R. E.; Miskowski, V. M.; Schaefer, W. P.; Gray, H. B. *Inorg. Chem.* **1995**, *34*, 4591.
(5) Samha, H.; Martinez, T.; De Armond, M. K. *Langmuir* **1992**, *8*, 2001.
(6) Samha, H.; De Armond, M. K. *Coord. Chem. Rev.* **1991**, *111*, 73.
(7) Neve, F.; Crispini, A.; Campagna, S. *Inorg. Chem.* **1997**, *36*, 6150.
(8) Kimizuka, N.; Oda, N.; Kunitake, T. *Chem. Lett.* **1998**, 695.
(9) (a) Yip, H.-K.; Che, C.-M.; Zhou, Z.-Y.; Mak, T. C. W. *J. Chem. Soc., Chem. Commun.* **1992**, 1369. (b) Tzeng, B.-C.; Fu, W.-F.; Che, C.-M.; Chao, H.-Y.; Cheung, K.-K.; Peng, S.-M. *J. Chem. Soc., Dalton Trans.* **1999**, 1017. (c) Lai, S.-W.; Chan, M. C. W.; Cheung, K.-K.; Che, C.-M. *Inorg. Chem.* **1999**, *38*, 4262.
(10) (a) Miskowski, V. M.; Houlding, V. H. *Inorg. Chem.* **1989**, *28*, 1529. (b) Miskowski, V. M.; Houlding, V. H. *Inorg. Chem.* **1991**, *30*, 4446.
(11) (a) Arena, G.; Calogero, G.; Campagna, S.; Scolaro, L.; Ricevuto, V.; Romeo, R. *Inorg. Chem.* **1998**, *37*, 2763. (b) Connick, W. B.; Geiger, D.; Eisenberg, R. *Inorg. Chem.* **1999**, *38*, 3264.
(12) Shih, K.-C.; Herher, R. H. *Inorg. Chem.* **1992**, *31*, 5444.
(13) Miskowski, V. M.; Houlding, V. H.; Che, C.-M.; Wang, Y. *Inorg. Chem.* **1993**, *32*, 2518.
(14) Kunkely, H.; Vogler, A. *J. Am. Chem. Soc.* **1990**, *112*, 5625.
(15) Cummings, S. D.; Eisenberg, R. *J. Am. Chem. Soc.* **1996**, *118*, 1949.
(16) Buchner, R.; Cunningham, C. T.; Field, J. S.; Haines, R. J.; McMillin, D. R.; Summerton, G. C. *J. Chem. Soc., Dalton Trans.* **1999**, 711.

10.1021/ic990880m CCC: $19.00
Published on Web 08/06/2000

Scheme 1. Molecular Structures of the L18 Ligand and the $[Pt(L18)Cl]^+$ Complex

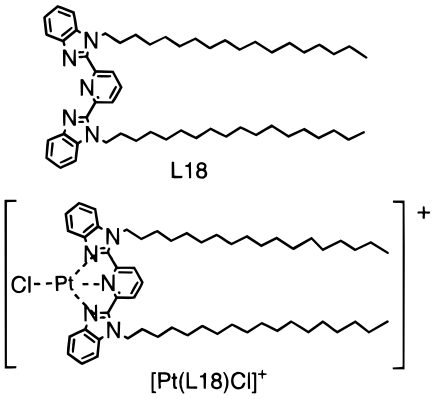

been shown to oligomerize in solution via weak metal−metal interactions.[17] The metal−metal interaction affects the energy levels of MLCT and MMLCT states and therefore changes the characteristics of excited states.[18] Recently, it has been reported that the electronic spectrum of [Pt(tpy)Cl]X (tpy = 2,2′:6′,2″-terpyridine) is influenced dramatically by intermolecular stacking interactions in both the fluid solution and the solid state.[4] The $[Pt(tpy)Cl]^+$ complex exhibits concentration-dependent absorption and emission spectra in solution. Furthermore, the solid-state properties of [Pt(tpy)Cl]X are highly dependent on the counterion X: i.e., an orange color in the solid state for the Cl^- and $CF_3SO_3^-$ salts and yellow for the PF_6^- salt. Therefore, the control of supramolecular structures, particularly for Pt−Pt interaction, is a prerequisite for tuning electronic properties of Pt complexes. From the studies on the metal coordination chemistry of the 2,6-bis(benzimidazol-2-yl)pyridine ligand, the similarity of coordination ability between 2,6-bis(benzimidazol-2-yl)pyridine and tpy has been pointed out.[19,20] The Pt complexes containing 2,6-bis(benzimidazol-2-yl)pyridine derivatives have not been reported, and therefore we comparatively investigate Pt complexes of 2,6-bis(benzimidazol-2-yl)pyridine (Scheme 1). In this paper, we report the preparation and properties of a novel Pt complex containing 2,6-bis(1-octadecylbenzimidazol-2-yl)pyridine (L18), particularly focusing on the intermolecular aggregation of the Pt−Pt interaction and molecular orientation both in solution and in LB films.

Experimental Section

Materials and General Methods. 1-Bromooctadecane (Nacalai) and potassium tetrachloroplatinate, K_2PtCl_4 (N. E. Chemcat), were used without further purification. Dichloromethane and chloroform were purified by distillation over P_2O_5. 2,6-Bis(benzimidazol-2-yl)pyridine and the L18 ligand were prepared by the methods given in the literature.[21−23] All other chemicals were of standard reagent grade.

Synthesis of the Pt Complex. [Pt(L18)Cl](PF$_6$). K_2PtCl_4 (0.15 g, 0.36 mmol) was dissolved in dimethyl sulfoxide (DMSO, 30 mL), and solid ligand L18 (0.3 g, 0.37 mmol) was added to the solution. The solution was heated for 10 h at 90 °C, during which time the color of the solution became orange. Upon cooling to room temperature, 10 mL of methanol was added and then the resulting solution was filtered. To the filtrate was added a saturated aqueous solution of NH_4PF_6 (5 mL) to precipitate the product. The color of the precipitate gradually turned from yellow to red. The red precipitate was collected by filtration and washed with water. Further purification was performed by recycling preparative HPLC LC-908 (JAI Co., Ltd.) with $CHCl_3$ as an eluent. Anal. Calcd for $C_{55}H_{85}N_5PtClPF_6$: C, 55.43; H, 7.19; N, 5.88. Found: C, 55.13; H, 7.31; N, 5.71. ESI-M:. 1046.8 ($[M - PF_6]^+$). ^1H NMR (400 MHz, DMSO-d_6): δ 8.61 (t, J = 7.9 Hz, 1H), 8.44 (d, J = 7.9 Hz, 2H), 8.40 (d, J = 8.3 Hz, 2H), 7.96 (d, J = 8.3 Hz, 2H), 7.61 (t, J = 8.3 Hz, 2H), 7.54 (t, J = 8.3 Hz, 2H), 4.81 (m, 4H), 1.87 (m, 4H), 1.4−1.2 (m, 60H), 0.84 (t, J = 8.2 Hz, 6H).

Physical Measurements. General Measurements. Electronic absorption spectra were obtained on a Hitachi U-4000 or a U3210 spectrophotometer. XPS spectra were measured on a VG Scientific ESCA Mark II photoelectron spectrometer with Mg Kα radiation as an excitation source. Binding energies of the peaks were referenced by the C 1s peak at 285.0 eV. Emission spectra of LB films were measured with a Jobin Yvon-Spex FluoroMax2 spectrofluorometer. Emission lifetime was measured by means of the single photon counting method on a Horiba NASE-550 nanosecond lifetime measurement system. NMR spectra were measured with a 400 MHz JEOL spectrometer. Electrospray mass spectrometric experiments were carried out with a model LCQ electrospray mass spectrometer (ESI-MS) (Finnigan MAT).

LB Film Preparation. Hydrophilic treatments of glass or quartz substrates were made by consecutive sonication of the substrate in detergent for 30 min and in $CHCl_3$/EtOH for 15 min and then soaking in piranha solution (30% H_2O:concentrated H_2SO_4 = 1:3 v/v) for 8 h, and finally washing repeatedly with copious ultrapure water before use. **CAUTION:** *Piranha solution reacts violently, even explosively, with organic materials, and it should not be stored in sealed containers or combined with significant quantities of organic material!* For all LB experiments, ultrapure water (≥18 MΩ cm^{-1}), which was purified by an Elgastat UHQ-III system (Kleiner, Switzerland), was used. The surface pressure−area measurements and film transfer experiments were carried out on a USI FSD-300 computer-controlled Langmuir trough (Teflon coating, effective area: 51.7 cm × 15 cm) with a Wilhelmy balance as a surface pressure sensor. This system was placed on a vibration-isolating table and was protected from dust by a plastic cover. A Pt complex solution (6.5 mg in 5 mL of $CHCl_3$) was spread onto a pure water subphase which was kept at a constant temperature of 20 ± 0.5 °C by a thermostat. After waiting for the evaporation of the solvent for 30 min, the surface pressure−area isotherms were recorded at a compression speed of 0.5 mm s^{-1}. For a compression−expansion experiment, expansion of monolayer was made immediately after the barrier reached to the preset surface pressure of compression at the same rate as the compressions (0.5 mm s^{-1}). Monolayer formed at the air−water surface was held at the constant pressures for 30 min for stabilization and then transferred to glass or quartz substrates at a vertical dipping rate of 5 mm min^{-1}.

In Situ UV−Vis Spectra of Monolayers on Subphase. In situ UV−vis spectra of monolayers on the pure water subphase were recorded on a UV−vis spectrophotometer (UNISOKU Ltd.) with a Hamamatsu R2949 photomultiplier and a Y-type quartz optical fiber, according to the reported apparatus configuration.[24] The spectrum was taken by light passing through the monolayer with an Al, Au, or Ag mirror placed about 5 mm under the water surface reflecting the signal vertically back, via a second pass through the monolayer, to the optical fiber probe. Unless otherwise mentioned, the incidence angle of the beam relative to the normal of the subphase surface is zero. For all measurements, monolayer-free subphase is used as a reference.

Results and Discussion

UV−Vis and Emission Spectra in Solution. Square-planar Pt(II) complexes with bidentate ligands such as 2,2′-bipyridine

(17) (a) Hill, M. G.; Bailey, J. A.; Miskowski, V. M.; Gray, H. B. *Inorg. Chem.* **1996**, *35*, 4585. (b) Sakai, K.; Takeshita, M.; Ue, T.; Yanagisawa, M.; Kosaka, M.; Tsubomura, T.; Ato, M.; Nakano, T. *J. Am. Chem. Soc.* **1998**, *120*, 11353.
(18) Wu, L.-Z.; Cheung, T.-C.; Che, C.-M.; Cheung, K.-K.; Lam, M. H. W. *Chem. Commun.* **1998**, 1127.
(19) Piguet, C.; Bocquet, B.; Muller, E.; Williams, A. F. *Helv. Chim. Acta* **1989**, *72*, 323.
(20) Addison, A. W.; Burman, S.; Wahlgren, C. G.; Rajan, O. A.; Rowe, T. M.; Sinn, E. *J. Chem. Soc., Dalton Trans.* **1987**, 2621.
(21) Xiaoming, X.; Haga, M.; Matsumura-Inoue, T.; Ru, Y.; Addison, A. W.; Kano, K. *J. Chem. Soc., Dalton Trans.* **1993**, 2477.
(22) Addison, A. W.; Burke, P. J. *J. Heterocycl. Chem.* **1981**, *18*, 803.
(23) Haga, M.; Kato, N.; Monjushiro, H.; Wang, K.; Hossain, M. D. *Supramol. Sci.* **1998**, *5*, 337.
(24) Ouyang, J.; Lever, A. B. P. *J. Phys. Chem.* **1991**, *95*, 5272.

and 1,10-phenanthroline or tridentate ligands such as tpy and its derivatives show varieties of colors from yellow to red in the solid state. Data have been compiled for the relationship between the intermolecular Pt−Pt interactions and the solid colors as well as the factors that govern stacking interactions.[25−29] The red-colored crystals are associated with the appearance of an absorption band at >500 nm, which originates from the Pt−Pt intermolecular interaction as verified by X-ray structural analyses. Such interaction is absent in the yellow form of crystals. The present Pt complex we studied has a red color, indicative of Pt−Pt interaction in the solid state. According to its color, [Pt(L18)Cl](PF_6) should have Pt−Pt interaction in the solid state.

The UV−vis spectrum of L18 displays one broad band centered at 322 nm (ϵ, 30300 mol^{-1} dm^3 cm^{-1}), which was assigned to the $\pi \rightarrow \pi^*$ transition as established for the short alkyl chain analogues of L18.[19,30,31] The red solid Pt complex [Pt(L18)Cl](PF_6) was dissolved in propylene carbonate (PC) to give a yellow solution. The UV spectra (1.0×10^{-5} M) (M = mol dm^{-3}) exhibits four peaks at $\lambda_{max} = 311$ (ϵ 25000 mol^{-1} dm^3 cm^{-1}), 341 (28000), 353 (22000), and 372 nm (25000) for the PC solution, and 317 (ϵ, 23200 mol^{-1} dm^3 cm^{-1}), 352 (21900), 363 (22000), and 382 nm (19200) for the $CHCl_3$ solution and were a little red-shifted relative to the PC solution. A little longer wavelength shift for each four peaks in $CHCl_3$ is notable. These peaks must be splitting components of the ligand $\pi \rightarrow \pi^*$ transitions. Similar splitting was observed previously for the Cu^{2+}, Cu^+, Zn^{2+}, and Fe^{2+} complexes with the methyl analogue of the ligand L18.[19,31] Substantial mixing of L18 π^* orbitals with the Pt $6p_z$ orbital most probably contributes to the different spectral patterns observed between the free ligand and the corresponding Pt complex. This is well supported by a rigorous study of these interactions in the [Pt(tpy)Cl]$^+$ complex.[17a] In the visible region, two weak peaks at 427 (ϵ, 1600 mol^{-1} dm^3 cm^{-1}) and 453 nm (1100) were observed, which were assigned to MLCT($d\pi-\pi^*$) transitions. The UV−vis absorption spectrum of [Pt(L18)Cl](PF_6) showed strong concentration dependence. Detailed concentration dependence was studied for the $CHCl_3$ solution. Below a concentration of 10^{-4} M, the spectra obeyed Lambert−Beer's law. The relative intensity of the peak at 317 nm increased with increasing complex concentration ($(1.0-10.0) \times 10^{-4}$ M), and the two peaks at 352 and 363 nm are mingled as one shoulder at 349 nm when the concentration is higher than 5.0×10^{-4} M. Above 10^{-4} M a new peak appeared at around 550 nm as shown in Figure 1. The concentration dependence is similar to that observed for [Pt(tpy)Cl]$^+$ and is associated with the increasing Pt−Pt interaction as well as ligand−ligand interaction at higher complex concentrations.[4] The band at 550 nm was thus assigned to ^{3}MMLCT transitions. No additional peaks at lower wavelength were observed on increasing the oncentration up to 10^{-3} M. Thus, the equilibrium moves to mainly the formation of dimeric species.

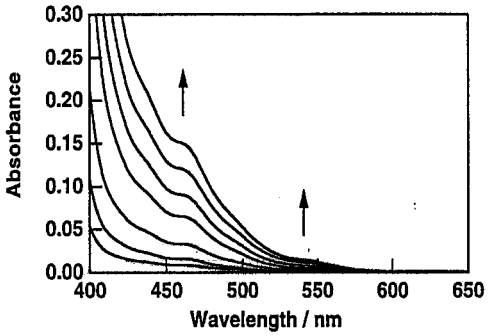

Figure 1. Concentration dependence of visible spectra of [Pt(L18)Cl]$^+$ in $CHCl_3$. From top to bottom: [Pt] = 1.8×10^{-4}, 1.46×10^{-4}, 9.2×10^{-5}, 6.3×10^{-5}, 3.3×10^{-5}, 1.1×10^{-5}, and 5.5×10^{-6} M.

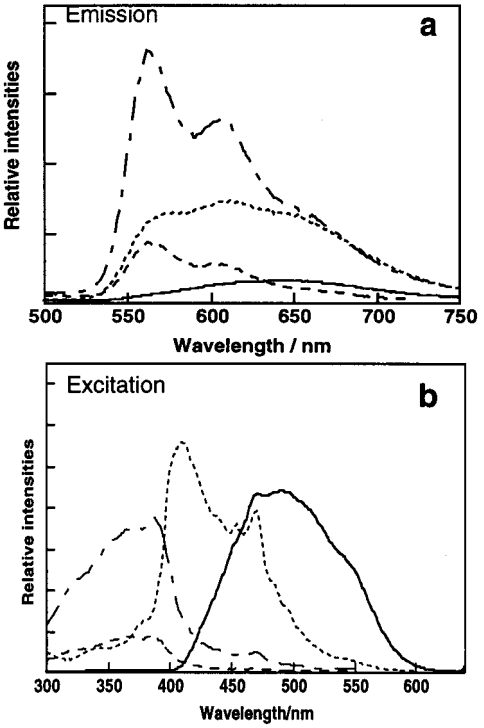

Figure 2. Concentration dependence of (a) emission spectra and (b) the corresponding excitation spectra of [Pt(L18)Cl]$^+$ in $CHCl_3$. [Pt] concentration: (a) [Pt] = 1.1×10^{-3} (—), 1.40×10^{-4} (···), and 1.1×10^{-5}M (—·—) and 1.1×10^{-6} (---) (excited at 380 nm). (b) [Pt] = 1.1×10^{-3} (—) 1.40×10^{-4} (···) (monitored at 650 nm), and 1.1×10^{-5}M (—·—) (monitored at 560 nm) and 1.1×10^{-6} (---) (monitored at 560 nm).

The emission spectra of [Pt(L18)Cl](PF_6) in both $CHCl_3$ and PC solutions also produced concentration dependence. Figure 2 shows the concentration dependence of emission and excitation spectra for the $CHCl_3$ solution. A dilute $CHCl_3$ solution of 1×10^{-5} M gave an emission spectrum at 564, 605, and 660 nm with vibronic progressions of ~1190 cm^{-1}, when excited at 380 nm. The excitation spectrum as monitored at 564 nm showed peaks at 382 and 465 nm. The emission spectrum at ~560 nm is similar to that of the methyl analogue.[32] Since the emission maxima of the free ligand appear in the higher energy region of ~384 nm (from the $^1\pi\pi^*$ state) and ~470 nm (from $^3\pi\pi^*$),[33] the emission of [Pt(L18)Cl](PF_6) in $CHCl_3$ is red-shifted with respect to that from pure ligand $^3\pi-\pi^*$ transitions. The emission maxima are slightly blue-shifted to 540 nm on lowering the

(25) Connick, W. B.; Marsh, R. E.; Schaefer, W. P.; Gray, H. B. *Inorg. Chem.* **1997**, *36*, 913.
(26) Canty, A. J.; Skelton, B. W.; Trail, P. R.; White, A. H. *Aust. J. Chem.* **1992**, *45*, 417.
(27) Osborn, R. H.; Rogers, D. *J. Chem. Soc., Dalton Trans.* **1974**, 1002.
(28) Herber, R. H.; Croft, M.; Coyer, M. J.; Bilash, B.; Sahiner, A. *Inorg. Chem.* **1994**, *33*, 2422.
(29) Kato, M. K. S.; Kosuge, C.; Yamazaki, M.; Yano, S.; Kimura, M. *Inorg. Chem.* **1996**, *35*, 116.
(30) Piguet, C.; Bernardinelli, G.; Williams, A. F. *Inorg. Chem.* **1989**, *28*, 2920.
(31) Ruttimann, S.; Piguet, C.; Bernardinelli, G.; Bocquet, B.; Williams, A. F. *J. Am. Chem. Soc.* **1992**, *114*, 4230.
(32) Akiba, M.; Sasaki, Y.; Haga, M. Unpublished data.
(33) Petoud, S.; Bunzli, J.-C. G.; Schenk, K. J.; Piguet, C. *Inorg. Chem.* **1997**, *36*, 1345.

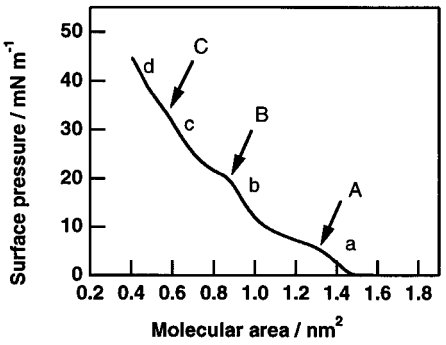

Figure 3. Surface pressure−molecular area isotherm of the [Pt(L18)Cl]$^+$ complex on a pure water subphase at 20 °C. The breaking points are marked A, B, and C, with arrows, and the linear regions are marked a, b, c, and d.

temperature from 297 to 80 K. From these results, the emission at ∼560 nm is tentatively assigned to metal-perturbed ligand-centered $^3\pi-\pi^*$ transitions. Similar metal-perturbed ligand-centered $^3\pi-\pi^*$ transitions were reported in [Pt(tpy)X] complexes.[11a,16] Molecular orbital calculation by Spartan provides lower HOMO and LUMO energies of 2,6-bis(1-methylbenzimidazol-2-yl)pyridine than those of tpy, which is consistent with the red shift of emission maxima for [Pt(L18)Cl](PF_6) compared to that for [Pt(tpy)Cl]. On increasing the concentration beyond 1×10^{-4} M, relative emission intensity around 650 nm increased, and the corresponding excitation spectrum as monitored at 650 nm showed a clear shoulder at 550 nm in addition to the maxima at 420 and 460 nm. When the solution (1.1×10^{-3} M) was excited at 550 nm, broad featureless emission with the maximum at 650 nm was observed. This lower energy emission band is thus associated with the ^{3}MMLCT transition. Similar concentration dependence of emission spectra was observed in PC solution. A difference between PC and $CHCl_3$ solutions was revealed from the emission lifetime measurements. The emission in PC (1×10^{-5} M) at room temperature decayed exponentially at each maximum with the identical lifetime of 0.550 μs, and the emission was clearly composed of a single component. However, the emission decay curve of well-aerated $CHCl_3$ solution (1×10^{-5} M) was found to be double components; the major component (85%) has a lifetime of 0.22 μs, while the minor component (15%) possesses a lifetime of 0.045 μs. The minor component may arise from a dimerization of the Pt complex formed in less polar $CHCl_3$ solution. An alternative explanation is that the emission arises from a excimer, resulting from association of an excited complex with a ground-state complex.[11b]

The red solid of [Pt(L18)Cl](PF_6) shows a broad emission band centered at around 650 nm, for which the excitation spectrum shows a maximum at 545 nm. The emission must be of ^{3}MMLCT origin.

Surface Pressure−Area Isotherm. The surface pressure−area isotherm for the Pt complex on a pure water subphase is shown in Figure 3. This isotherm is reproducible. Three phase transitions were consecutively observed as breaking points which are marked with A, B, and C in Figure 3, respectively. Limiting molecular areas at four regions a, b, c, and d in Figure 3 were derived to be 1.45, 1.18, 1.06, and 0.95 nm^2, by the extrapolation of four linear regions 1−6, 12−20, 25−33, and 37−45 mN of the isotherm to a zero surface pressure, respectively. Two possible orientations of the square-planar Pt complex are "side-on" and "flat-on" fashions on the air−water interface. The "side-on" orientation,which refers to the vertical orientation of the Pt chromophore plane with respect to the air−water interface,

Scheme 2. Three Possible Molecular Packing Modes of the [Pt(L18)Cl]$^+$ Complex on the Air−Water Interface[a]

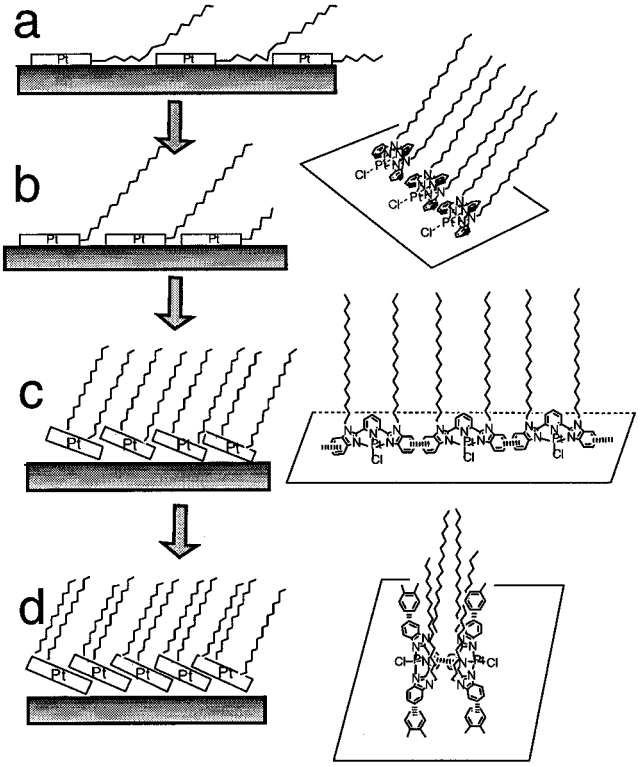

[a] Dashed lines show $\pi-\pi$ interactions. The symbols a, b, c, and d in the scheme correspond to the proposed molecular packing in Figure 3.

should lead to a molecular occupied area of 0.43 nm^2 (1.2 nm × 0.36 nm). Since all the molecular areas observed here are much larger than this value, the "side-on" orientation could be excluded on the air−water interface. The molecular area of 1.45 nm^2 for the first phase, phase a, is even larger than the molecular area of 1.18 nm^2, which is predicted for the "flat-on" orientation of the Pt complex chromophore plane: 0.78 nm^2 (1.2 nm × 0.64 nm) of the Pt plane plus smallest occupied area of 0.4 nm^2 for two alkyl chains. Therefore, the first linear region of the $\pi-A$ curve with the largest limiting molecular area is ascribed to a liquid-expanding region. At this area, the molecules are loosely packed and alkyl chains lie with a large tilt to the normal of the air−water interface. This large tilt of alkyl chains and the mutual separation of the Pt molecules contribute to the large molecular area observed. Following the liquid-expanding region, a solid-condensed region was observed, in which the molecules form a closely packed monolayer of the "flat-on" orientation with the molecular area of 1.18 nm^2. If the coordination planes were almost completely stacked to each other upon further compression, the molecular area should decrease dramatically. While the observed limiting molecular areas differ only by 0.11−0.12 nm^2 between the linear regions b and c, and the regions c and d, it is conceivable that the coordination planes between adjacent Pt complexes are only partially stacked. Since the area difference of 0.12 nm^2 is close to the occupied area of a benzene or pyridine ring, the orientations for the third and fourth linear regions involve partial $\pi-\pi$ stacking of benzene rings and pyridyl ones in two adjacent Pt complexes, respectively. The proposed molecular packing for regions a−d is schematically depicted in Scheme 2.

The reversibility of the compression−expansion isotherms of the monolayer film was measured as shown in Figure 4. When the monolayer was compressed to the surface pressure

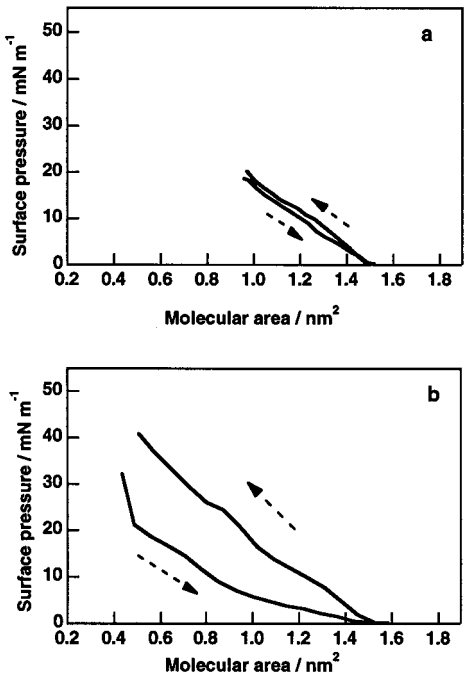

Figure 4. Compression−expansion surface pressure−area isotherms of the $[Pt(L18)Cl]^+$ complex on pure water at reversal pressures of (a) 20 mN m^{-1} and (b) 40 mN m^{-1}.

of 20 mN m^{-1} and then subsequently expanded, a small hysteresis was observed (Figure 4a). This result indicates that the compression and expansion processes are quasi-reversible, which is characteristic of a closely packed monolayer. On the other hand, the expansion of the monolayer at the reversal pressure of 40 mN m^{-1} revealed a large hysteresis (Figure 4b), supporting the presence of strong intermolecular interaction like $\pi-\pi$ interaction as we addressed above. Steric hindrance of the long alkyl chains and strong hydrophobicity around the Pt ion make it difficult to stack the planar $[Pt(L18)Cl](PF_6)$ complexes at the air−water interface. Our assumption of partial $\pi-\pi$ stacking of two adjacent molecules on the water surface was also supported by the crystal structures of many related Pt(II) α,α′-diimine and tpy complexes, e.g., diphenyltriazenido-Pt(tpy)[34] and $PtCl_2$(i-biq),[29] in which i-biq is 3,3′-biisoquinoline. In these crystals, the complexes adopt a slipped stack structure, keeping van der Waals contacts between parts of the adjacent π acceptors.

LB Film Transfer onto Solid Substrate. Four different surface pressures at 5, 15, 25, and 35 mN m^{-1}, which correspond to different linear regions in the $\pi-A$ curve, were chosen for LB transfer onto a solid substrate. For each case, the LB film transfer was made by the vertical dipping method on both up- and downstrokes for a typical Y-type deposition, i.e., head-to-head and tail-to-tail fashion. In order to transfer the monolayer from water surface onto the substrate smoothly, the barrier should be held for 30 min at the target pressures prior to the film transfer. At the initial period on the compression, the surface pressure largely fluctuates until an energetically favorable orientation is attained since the intermolecular interaction made the molecules reorient. Therefore, we found that this procedure was particularly important when high target pressures of 25 and 35 mN m^{-1} were used. At the lowest pressure of 5 mN m^{-1}, only monolayer LB transfer could be achieved, and further attempts to prepare multilayers by changing the experimental

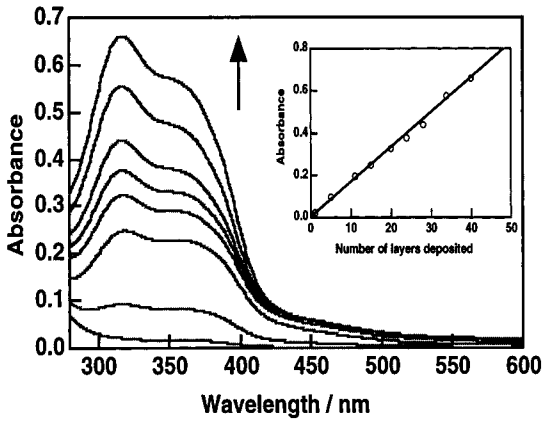

Figure 5. UV spectra of $[Pt(L18)Cl]^+$ LB films of varied numbers of layers deposited on a glass plate at a surface pressure of 25 mN m^{-1} (from bottom to top: 1, 5, 15, 21, 25, 29, 35, and 41 layers). The plot of absorbance at 318 nm vs the number of layers is shown as an inset.

parameters, e.g., deposition rate and drying time of the film after finishing the first upstroke from the subphase, were unsuccessful. On the other hand, at the other three surface pressures of 15, 25, and 35 mN m^{-1}, multilayer films were successfully formed onto the glass or quartz substrate with mean transfer ratios of 0.9−1.1 in a layer-by-layer fashion. Furthermore, the deposition process onto a glass plate at the surface presure of 25 mN m^{-1} was monitored by UV spectra (Figure 5). The plot of absorbance vs the number of layers displays a straight line as shown in the inset of Figure 5, which reveals successful multilayer formation of LB film. Similar straight lines for the plots of absorbance vs number of layers were obtained at the other surface pressures of 15 and 35 mN m^{-1}, respectively.

Low-Angle X-ray Diffraction. In order to evaluate the molecular ordering and estimate the molecular orientation in LB films on solid substrates, low-angle X-ray diffraction was run on a 25-layer Y-type LB film prepared at 15 mN m^{-1}. A sharp (001) Bragg diffraction was observed at $2\theta = 2.76°$, suggesting an ordered structure of the LB film with a bilayer spacing of 3.2 nm. This value is much smaller than the 4.4 nm obtained from molecular modeling for the "flat-on" orientation on the air−water interface. Obviously, the long alkyl chains are tilted from the normal of the glass substrate after the transfer. This kind of molecular relaxing is often observed when the molecules are transferred from water surface to a solid substrate.

X-ray Photoelectron Spectroscopy. Figure 6 shows the XPS core level spectra for a 23-layer Pt complex LB film transferred at 15 mN m^{-1} on a glass plate. The XPS wide-scan spectrum gave characteristic elemental signatures for C 1s, Pt 4f, N ls, P 2p, Cl 2p, and F 1s lines, which agree with the chemical formula of $[Pt(L18)Cl](PF_6)$. In the high-resolution spectra the Pt $4f_{5/2}$ and Pt $4f_{7/2}$ signals were observed at 73.8 and 77.1 eV, respectively, which are typical values for Pt(II) complexes.[35] Angular-resolved Pt 4f, Cl 2p, and N 1s spectra show little angular dependence, giving additional support for the "flat-on" orientation of Pt complex LB films on the hydrophilic glass surface.

UV Spectra of LB Films. Surface pressure dependent in situ UV−visible spectra of the monolayer formed at the air−water interface are shown in Figure 7. Two peaks at 315 and 369 nm were observed regardless of the surface pressures. The former absorption maximum is almost the same as that in PC or $CHCl_3$ solution, and the latter one is essentially the collapse of three

(34) Bailey, J. A.; Catalano, V. J.; Gray, H. B. *Acta Crystallogr.* **1993**, *C49*, 1598.

(35) Burroughs, P.; Hamnett, A.; McGilp, J. F.; Orchard, A. F. *J. Chem. Soc., Faraday Trans. 2* **1975**, *71*, 177.

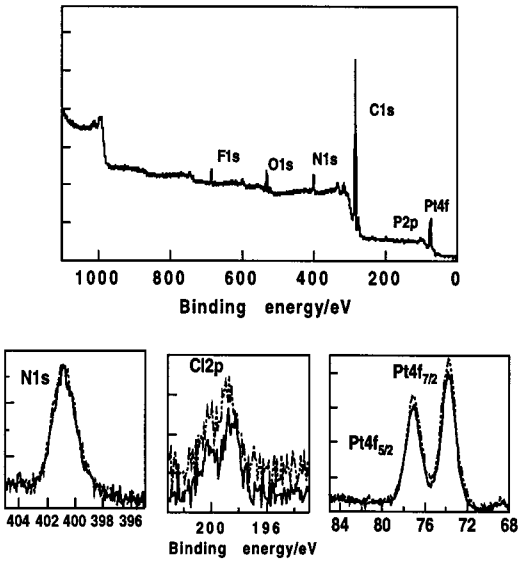

Figure 6. XPS wide-scan spectrum for a 23-layer $[Pt(L18)Cl]^+$ LB film on a glass plate transferred at 15 mN m^{-1}, and high-resolution spectra of N 1s, Cl 2p, and Pt 4f regions measured at detection angles of 10° (solid line) and 65° (dashed line) with respect to the surface normal.

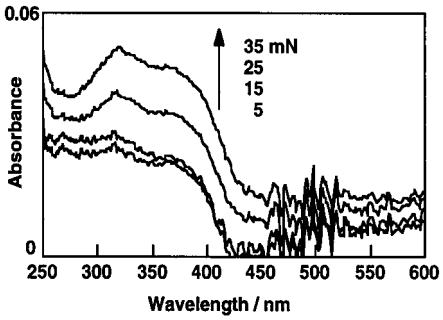

Figure 7. In situ UV−vis spectra of a $[Pt(L18)Cl]^+$ monolayer film on pure water at the surface pressures of 5, 15, 25, and 35 mN m^{-1}.

peaks at 341, 353, and 372 nm observed in PC. It is noteworthy that the relative intensity of the absorption peak at 315 nm compared to that at 369 nm increases when the surface pressure increases from 5 to 35 mN m^{-1}. A similar enhancement was observed in PC and $CHCl_3$ solution of the Pt complex at higher concentrations. Thus the enhancement in the relative intensity of the peak at 315 nm supports the mixing of π orbitals through intermolecular $\pi-\pi$ interactions between Pt complexes.

The plots of absorbance for the transferred LB film on the glass substrate vs number of layers gave straight lines. This indicates that the Pt complex forms stable LB multilayer films. Two broad absorption bands were observed at 318 and 370 nm. During the multilayer LB deposition on glass, the relative intensity of the peak at 318 nm for the LB films with respect to the shoulder at 370 nm slightly increases with increasing the number of layers (Figure 5), which suggests the presence of weak interlayer intermolecular interaction in the Y-type LB films.

Emission Spectra of LB Films. Figure 8 shows four emission spectra (excitation wavelength 368 nm) of monolayer LB films on glass substrates prepared at different surface pressures of 5, 15, 25, and 35 mN m^{-1}. With increasing the surface pressure, the emission maxima move from 560 to 600 nm. The LB monolayer films at 5 and 15 mN m^{-1} exhibit the emission maxima at 560 and 590 nm, which can be assigned to metal-perturbed ligand-centered $^3\pi-\pi^*$ transitions. The excitation

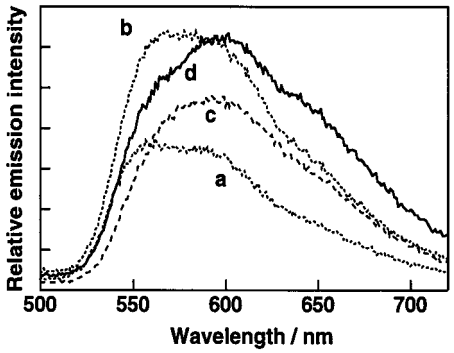

Figure 8. Dependence of emission spectra of $[Pt(L18)Cl]^+$ LB monolayer films on transferred surface pressures of (a) 5, (b) 15, (c) 25, and (d) 35 mN m^{-1} (excitation wavelength = 368 nm) on glass substrates.

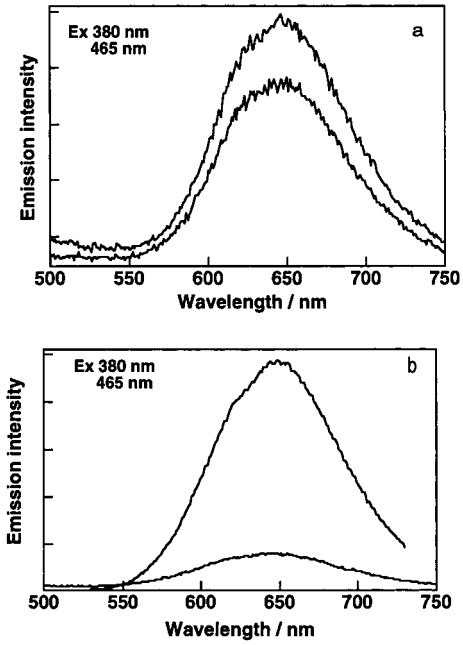

Figure 9. Emission spectra of $[Pt(L18)Cl]^+$: (a) solid state and (b) cast films at two different excitation wavelengths.

spectra of the *monolayer* films exhibit two bands at 369 and 465 nm. Above the surface pressure of 15 mN m^{-1}, the emission maximum is shifted to a longer wavelength (600 nm). When excited at 465 nm, these four films show a broad weak symmetrical emission band around 580−600 nm, which is mainly due to a ligand−ligand $\pi-\pi$ interacted excited state as a result of intermolecular ligand−ligand interaction. However, no detectable emission was observed when the LB *monolayer* film was excited at 550 nm, which corresponds to the MMLCT transition in PC or $CHCl_3$ solution. Nevertheless, this fact does not warrant the conclusion that Pt−Pt interaction does not exist in the LB films since we cannot exclude the possibility that the weak emission exceeds a detect limit of the apparatus. Consequently, a monomer emission at 560 nm arising from metal-perturbed ligand-centered $^3\pi-\pi^*$ transitions was observed at lower surface pressure (below 15 mN m^{-1}). On increasing the surface pressure above 15 mN m^{-1}, partial $\pi-\pi$ stacking of benzene rings and pyridyl ones in two adjacent Pt complexes leads to a new ligand−ligand $\pi-\pi$ interacted excited state exhibiting the emission at 600 nm; on the other hand, the emission at 650 nm arising from Pt−Pt interacted MMLCT states is hardly observed.

Emission spectra of multilayer films are more complex than the emission spectra of monolayer films but clearly show no MMLCT emission band at about 650 nm. However, after storage at room temperature for 4 months, the multilayer films of a 24-layer LB film prepared at $\pi = 25$ mN m^{-1} emit predominantly at 650 nm, which is nearly the same as the emission maximum of the red solid sample of the Pt complex. The emission spectrum of the coated film by the simple evaporation of the Pt complex in $CHCl_3$ solution similarly exhibits a band at 650 nm. (Figure 9). These results strongly suggest that Pt−Pt interactions were greatly suppressed in the LB film unless the film deteriorated. The Pt complexes in the high-concentrated solution, solid, and coated film have a strong tendency of self-stacking with Pt−Pt interactions. In the freshly prepared ordered LB film, the Pt−Pt interaction is largely suppressed.

Conclusion

The newly synthesized amphiphilic Pt complex itself shows stable and reproducible LB film-forming behavior without addition of auxiliary film-forming fatty acids. Strong emission from the LB films, even monolayer films, was observed. The detailed UV and emission spectral studies show that Pt−Pt interaction is greatly suppressed in the Langmuir monolayer film on the water surface and transferred LB films. The results would provide an insight into future Pt complex-based molecular devices from viewpoints of emission, charge transport, and electrical conductivity.

Acknowledgment. M.H. gratefully acknowledges financial supports from the Ministry of Education, Science, Culture and Sports for a Grant-in-Aid for Scientific Research (No. 09440233 and 12440188) and for Scientific Research on Priority Area of "Metal-assembled Complexes" (10149101). Support from the Grant for JSPS Fellows to K.Z.W. is also acknowledged.

IC990880M